Description of Scattering Object

A homogeneous low-loss dielectric plate of size $W \times 7W/4 \times 1.5$ mm.

Length Scale and Frequency Range

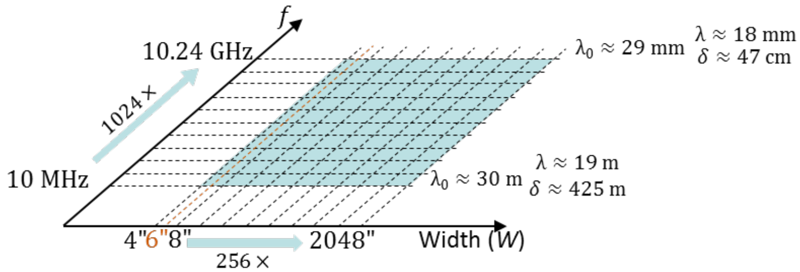

The problems of interest cover a range of 512x in physical length scale and 1024x in frequency; the ranges are logarithmically sampled to yield 110 + 12 scattering problems. In these problems, the plate sizes are in the range $0.0033 \leq W/\lambda_0 \leq 1776$ and $2.4 \times 10^{-4} \leq W/\delta \leq 111$, where λ_0 is the free-space wavelength and δ is the penetration depth in the dielectric. The length and width of the plates were chosen to approximately match the plate targets in [1], while the thickness was chosen to match that of Problem Set IID-Thin MagRAM Plates.

Interesting Features

1. The logarithmic sampling is distorted along the length axis and an extra plate of $W = 6$ in is introduced because of publicly available measurement data corresponding to this size [2]. The sampling is also distorted along the frequency axis: scattering from the plate of $W = 6$ in at frequencies $f \in$ {10, 20, 40, 80, 160, 320, 640, 1280, 2560, 5120, 7000, 10240} MHz are included in the problem set because of publicly available measurement data [2]. These distortions add 12 unique scattering problems to the set.
2. The thin side wall presents meshing and accurate integration challenges.
3. The low-loss dielectric material introduces extra uncertainties and sensitivities to RCS measurements and simulations [3].

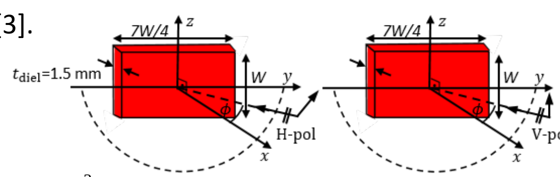

Quantities of Interest

Radar cross section (RCS) definition

$$\sigma_{vu}\left(\theta^{\mathrm{s}},\phi^{\mathrm{s}},\theta^{\mathrm{i}},\phi^{\mathrm{i}}\right)=\lim_{R\to\infty}4\pi R^2\frac{\left|\hat{v}\left(\theta^{\mathrm{s}},\phi^{\mathrm{s}}\right)\bullet\mathbf{E}^{\mathrm{scat}}\left(\theta^{\mathrm{s}},\phi^{\mathrm{s}}\right)\right|^2}{\left|\hat{u}\left(\theta^{\mathrm{i}},\phi^{\mathrm{i}}\right)\bullet\mathbf{E}^{\mathrm{inc}}\left(\theta^{\mathrm{i}},\phi^{\mathrm{i}}\right)\right|^2} \quad : \text{ RCS } (\mathrm{m}^2)$$

$$\sigma_{vu,\mathrm{dB}}\left(\theta^{\mathrm{s}},\phi^{\mathrm{s}},\theta^{\mathrm{i}},\phi^{\mathrm{i}}\right)=10\log_{10}\sigma_{vu} \quad : \text{RCS in dB (dBsm)}$$

$$\sigma^{TH}_{vu,\mathrm{dB}}\left(\theta^{\mathrm{s}},\phi^{\mathrm{s}},\theta^{\mathrm{i}},\phi^{\mathrm{i}}\right)=\max(\sigma_{vu,\mathrm{dB}},TH_{vu,\mathrm{dB}})-TH_{vu,\mathrm{dB}} \quad : \text{Thresholded RCS}$$

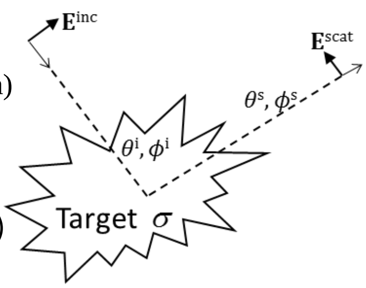

1. Set $\theta^{\mathrm{i}} = 90^{\mathrm{o}}$. Vary $0^{\mathrm{o}} \leq \phi^{\mathrm{i}} \leq 90^{\mathrm{o}}$ (every 0.5^{o} in the interval).
2. Compute back-scattered $\sigma_{\theta\theta,\mathrm{dB}}$ and $\sigma_{\phi\phi,\mathrm{dB}}$ (the VV- and HH-RCS in dB) at $N_\phi = 181$ scattering directions.

Material Properties

The permeability of the dielectric is the same as that of free space. A Debye model expressed as $\epsilon(f) = \epsilon_0 \varepsilon_r(f)$, where

$$\varepsilon_r(f) = \varepsilon_r'(f) - j\varepsilon_r''(f) = 2.6099 - j0.03778 + \frac{0.00203 + j0.00144}{1 - jf(0.01298 - j0.0641)}$$

was used to calculate the complex permittivity at the frequencies of interest. The reference simulation results were computed using precisely the permittivity values (i.e., to machine precision) shown in the below table. The above Debye model for the dielectric is the same as that in [2].

Frequency f (MHz)	ϵ'	ϵ''	Frequency f (MHz)	ϵ'	ϵ''
10	2.61	3.63×10^{-2}	2560	2.61	3.60×10^{-2}
20	2.61	3.63×10^{-2}	5120	2.61	3.54×10^{-2}
40	2.61	3.63×10^{-2}	7000	2.61	3.46×10^{-2}
80	2.61	3.63×10^{-2}	10 240	2.61	3.21×10^{-2}
160	2.61	3.63×10^{-2}			
320	2.61	3.63×10^{-2}			
640	2.61	3.63×10^{-2}			
1280	2.61	3.62×10^{-2}			

Performance Measures

Error Measure: Simulation errors shall be quantified using

$$avg.err_{uu,\mathrm{dB}}^{TH} = \frac{1}{2\pi}\int_0^{2\pi}\left|\sigma_{uu,\mathrm{dB}}^{TH}\left(\phi^{\mathrm{s}}\right) - \sigma_{uu,\mathrm{dB}}^{\mathrm{ref},TH}\left(\phi^{\mathrm{s}}\right)\right| d\phi^{\mathrm{s}} \approx \frac{1}{N_\phi}\sum_{n=1}^{N_\phi}\left|\sigma_{uu,\mathrm{dB}}^{TH}\left(\phi^{\mathrm{s}}\right) - \sigma_{uu,\mathrm{dB}}^{\mathrm{ref},TH}\left(\phi^{\mathrm{s}}\right)\right| \ (\mathrm{dB}) \ \text{ for } u \in \{\theta, \phi\}$$

where

$$TH_{uu,\mathrm{dB}} = \max_{\phi^s} \sigma_{uu,\mathrm{dB}}^{\mathrm{ref}} - 80 \ (\mathrm{dB})$$

This error measure discounts errors in RCS values below TH .

Cost Measure: Simulation costs shall be quantified using observed wall-clock time and peak memory/core

$t_{\mathrm{main}}^{\mathrm{wall}}$ (s) and $mem_{\mathrm{main}}^{\mathrm{maxcore}}$ (bytes)

as well as the "serialized" CPU time and total memory requirement

$t_{\mathrm{main}}^{\mathrm{total}} = N_{\mathrm{proc}} \times t_{\mathrm{main}}^{\mathrm{wall}}$ (s) and $mem_{\mathrm{main}}^{\mathrm{max}} = N_{\mathrm{proc}} \times mem_{\mathrm{main}}^{\mathrm{maxcore}}$ (bytes)

Here, N_{proc} denotes the number of processes used in a parallel simulation. It is expected that results will be reported for at least 2 runs: "Efficient" (small N_{proc}) and "Fast" (large N_{proc}).

Study 1: Error vs. Cost Sweep

Fix frequency and fix plate dimensions. Simulate many error levels (proxy: mesh densities) for 4 cases:

Case 1: *f*=10 MHz, *W*=6 in
Case 2: *f*=7 GHz, *W*=6 in (a measurement frequency)
Case 3: *f*=10 MHz, *W*=128 in
Case 4: *f*=320 MHz, *W*=128 in

It's recommended to simulate as many error levels (mesh densities) as possible. 3-5 error levels is typical. A typical error-vs.-cost study will consist of 4x3-5=12-20 simulations.

Study 2: Frequency Sweep

Fix plate dimensions and error level (proxy: mesh density). Simulate many frequencies for 4 cases:

Case 1: *W*=6 in, error level 1 (coarsest mesh)
Case 2: *W*=128 in, error level 1 (coarsest mesh)
Case 3: *W*=6 in, error level 2 (finer mesh)
Case 4: *W*=128 in, error level 2 (finer mesh)

Frequencies shall be chosen as $f \in \{10, 20, 40, \dots, 5120, 10240\}$ MHz. It's recommended to simulate as many frequencies as possible. A full frequency-sweep study will consist of 4x11=44 simulations.

Study 3: Size Sweep

Fix frequency and error level (proxy: mesh density). Simulate many sizes for 4 cases:

Case 1: *f*=10 MHz, error level 1 (coarsest mesh)
Case 2: *f*=320 MHz, error level 1 (coarsest mesh)
Case 3: *f*=10 MHz, error level 2 (finer mesh)
Case 4: *f*=320 MHz, error level 2 (finer mesh)

Dimensions shall be chosen as $W \in \{4, 8, 16, \dots, 1024, 2048\}$ in. It's recommended to simulate as many sizes as possible. A full size-sweep study will consist of 4x10=40 simulations.

Reference Quantities of Interest

The following RCS data are made available in the benchmark to enable participants to calibrate their simulators:

4 RCS measurement results corresponding to the W=6 in plate at frequencies $f \in \{2560, 5120, 7000, 10240\}$ MHz. The HH-polarized data are the same as those plotted in Fig. 7 of [2]; they are provided for ϕ^{i} sampled every 0.25$^{\mathrm{o}}$.

4 RCS simulation results for the W=6 in plate at the above 4 frequencies found by using the ARCHIE-AIM code, a frequency-domain FFT-accelerated integral-equation solver developed at UT Austin [4]-[6].

References

[1] A. C. Woo, H. T. G. Wang, M. J. Schuh and M. L. Sanders, “EM programmer's notebook-benchmark radar targets for the validation of computational electromagnetics programs,” *IEEE Ant. Propag. Soc. Mag.*, vol. 35, no. 1, pp. 84-89, Feb. 1993.

[2] J. T. Kelley, D. A. Chamulak, C. Courtney, and A. E. Yilmaz, “Increasing the material diversity in the Austin RCS Benchmark Suite using thin plates,” in *Proc. Ant. Meas. Tech. Assoc. (AMTA) Symp.*, Nov. 2020.

[3] J. T. Kelley, A. E. Yilmaz, D. A. Chamulak, and C. C. Courtney, “Measurements of non-metallic targets for the Austin RCS benchmark suite,” in *Proc. Ant. Meas. Tech. Assoc. (AMTA) Symp.*, Oct. 2019.

[4] M. F. Wu, G. Kaur, and A. E. Yılmaz, “A multiple-grid adaptive integral method for multi-region problems,” *IEEE Trans. Antennas Propag.*, vol. 58, no. 5, pp. 1601-1613, May 2010.

[5] F. Wei and A. E. Yılmaz, “A more scalable and efficient parallelization of the adaptive integral method part I: algorithm,” *IEEE Trans. Antennas Propag.*, vol. 62, no.2, pp. 714-726, Feb. 2014.

[6] J. W. Massey, V. Subramanian, C. Liu, and A. E. Yılmaz, “Analyzing UHF band antennas near humans with a fast integral-equation method,” in *Proc. EUCAP*, Apr. 2016.